Lawrence Berkeley National Laboratory

Lawrence Berkeley National Laboratory

Title

Inverse hydrochemical models of aqueous extracts tests

Permalink

https://escholarship.org/uc/item/91t6g5wc

Author

Zheng, L.

Publication Date

2008-11-15

Peer reviewed

eScholarship.org Powered by the California Digital Library
University of California

Inverse hydrochemical models of aqueous extracts tests

Liange Zheng [a], Javier Samper[*], Luis Montenegro

ETS Ingenieros de Caminos, Canales y Puertos, Campus de Elviña s/n, 15192 Universidad de Coruña. Coruña, Spain.

[a] Now at Lawrence Berkeley National Lab, 1 Cyclotron Road, Berkeley, CA, 94720, USA.

* Corresponding author. jsamper@udc.es (Tel.: +34-981-167-000; fax: +34-981-167-170)

Abstract

Aqueous extract test is a laboratory technique commonly used to measure the amount of soluble salts of a soil sample after adding a known mass of distilled water. Measured aqueous extract data have to be re-interpreted in order to infer porewater chemical composition of the sample because porewater chemistry changes significantly due to dilution and chemical reactions which take place during extraction. Here we present an inverse hydrochemical model to estimate porewater chemical composition from measured water content, aqueous extract, and mineralogical data. The model accounts for acid-base, redox, aqueous complexation, mineral dissolution/precipitation, gas dissolution/ex-solution, cation exchange and surface complexation reactions, of which are assumed to take place at local equilibrium. It has been solved with INVERSE-CORE^{2D} and been tested with bentonite samples taken from FEBEX (Full-scale Engineered Barrier EXperiment) *in situ* test. The inverse model reproduces most of the measured aqueous data except bicarbonate and provides an effective, flexible and comprehensive method to estimate porewater chemical composition of clays. Main uncertainties are related to kinetic calcite dissolution and variations in CO_2(g) pressure.

Keywords: aqueous extract, clay, porewater chemistry, hydrochemical model, inverse model, FEBEX bentonite, in situ test.

1. Introduction

Clay formations have been selected by several countries as candidate host rocks for high level radioactive waste (HLW) disposal in deep geological repositories and swelling clays used in as engineered barriers of such repositories (Alonso and Ledesma, 2005). Assessing the long-term safety of a HLW disposal site requires knowing the chemistry of clay porewater.

There are numerous experimental studies of water-clay interactions (Fritz and Kam, 1985; Wanner *et al.*, 1994; Cuevas *et al.*, 1997; Kraepiel *et al.*, 1998; Muurinen and Lehikoinen, 1999; Bradbury and Baeyens, 2003; Fernández *et al.*, 2004; Muurinen *et al.*, 2004). Geochemical modelling of porewater in clays is an active field of work where several approaches are taken to understand and quantify processes controlling porewater chemistry and its evolution in response to changes in environmental conditions (Wieland *et al.*, 1994; Beaucaire *et al.*, 2000; Bradbury and Baeyens, 1998, 2003; Muurinen and Lehikoinen, 1999; Arcos *et al.*, 2003; Fernández *et al.*, 2004; Pearson *et al.*, 2003; Wersin, 2003; Metz *et al.*, 2003; Ochs *et al.*, 2004; Wersin *et al.*, 2004; Samper *et al.*, 2005; Gaucher *et al.*, 2006; Turrero *et al.*, 2006; Sasamoto *et al.*, 2007). Geochemical evolution of clay porewater chemistry is controlled by cation exchange, proton surface complexation and dissolution/precipitation of soluble accessory minerals, and depends on ambient temperature and pressure as well as on solid-to-liquid ratio, *S/L* (Wanner *et al.*, 1994; Fernández *et al.*, 2004; Bradbury and Baeyens, 2003; Wersin, 2003; Wersin *et al.*, 2004).

Obtaining reliable data for clay porewater chemistry is a difficult task. Geochemical characterization of clays can be performed *in situ* by drilling and field techniques and *ex situ* by means of rock sampling, storage, preservation and laboratory analysis. There are numerous laboratory techniques to extract water from clay samples, such as centrifugation, squeezing, aqueous extraction or leaching, vacuum, azeotropic distillation and direct equilibration (Sacchi *et al.*, 2001). Squeezing and aqueous extract are the most commonly used methods. A large effort has been made during recent years to improve water extraction methods, develop numerical interpretation methods and achieve consistency between analytical data obtained from squeezing and aqueous extracts tests (Sacchi *et al.*, 2001; Bradbury and Baeyens, 2003; Pearson *et al.*, 2003). Both squeezing and aqueous extract alter the water-clay system in several ways and introduce sampling artefacts in measured data. Squeezing at high pressures may induce oxidation and dissolution of clay accessory minerals, outgassing of CO_2 and chemical fractionation (Sacchi *et al.*, 2001; Pearson *et al.* 2003). Furthermore, squeezing does not allow extracting porewater from clay samples with water contents less than 20% (Fernández *et al.*, 2004). For low water contents one must resort to aqueous extract tests (AET) in which a crushed sample is placed in contact with deionised water at a given *S/L* ratio. After establishing equilibrium, the solid phase is separated and the liquid phase is analyzed (Parshiva-Murthy and Ferrel, 1972, 1973). Since AET may alter the geochemical system, indirect hydrogeochemical modelling is needed to infer the chemical composition of porewater from AET data.

Here we present an inverse hydrochemical model for the interpretation of AET. Porewater composition of the clay sample is obtained by an inverse hydrogeochemical model using the inverse reactive transport code INVERSE-CORE^{2D} of Dai and Samper (2004). The paper starts with a description of AET and chemical processes which may occur during AET. After that, the inverse methodology is described. The inverse hydrochemical model is used to

interpret AET performed on bentonite samples taken from FEBEX *in situ* test at Grimsel (Switzerland). The paper ends with a discussion of main uncertainties and conclusions.

2. Aqueous extract test

2.1. Description

AET is a method to quantify the total content of soluble salts of a clay sample. An *1:R* aqueous extract test consists on adding to a mass M_s of powdered clay sample a mass of distilled water equal to R times M_s. Clay sample and water are stirred during a period of time of usually 2 days during which equilibration of water and clay sample is allowed. Chemical analyses are performed on supernatant solution after phase separation by centrifugation (Sacchi *et al.*, 2001). The solid-to-liquid ratio, *S/L*, is related to the aqueous extract ratio R through:

$$\frac{S}{L} = \frac{1}{w_i + R(1+w_i)} \tag{1}$$

where w_i is gravimetric water content of clay sample. It should be noticed that S/L coincides with 1/R only when clay sample is fully dry ($w_i = 0$). In addition to dilution, various chemical processes may occur during porewater extraction such as dissolution of soluble minerals (halite, sulphates and carbonates), dissolution and ex-solution of gases, cation exchange and surface complexation. All these processes perturb concentrations of dissolved species in a complex manner making difficult to derive the chemical composition of the original (before aqueous extraction) clay porewater from aqueous extract data. For this reason, aqueous extract data are mostly used to: 1) Evaluate the amount of soluble salts, 2) Derive concentrations of conservative species such as chloride and 3) Derive qualitative patterns for reactive species.

2.2. Interpretation

Concentration of a conservative species in the original clay porewater (before aqueous extraction), c_i, can be derived from concentration of aqueous extract, c_{ae}, performed on a clay sample of mass M_s from species mass balance

$$c_i w_i M_s = c_{ae} w_{ae} M_s \tag{2}$$

where w_{ae} is the gravimetric water content of the aqueous extract which is related to w_i through

$$w_{ae} = w_i + R(w_i + 1) \tag{3}$$

Substitution of Equation (3) into (2) leads to the expression of the dilution factor F

$$F = \frac{c_i}{c_{ea}} = 1 + R + \frac{R}{w_i} \tag{4}$$

which is equal to the ratio of concentrations of the original sample, c_i, and that of the aqueous extract, c_{ae}.

Inferring dissolved concentrations of reactive species requires geochemical modelling based on mineralogical data. Our methodology to infer clay porewater chemical composition from aqueous extract data is based on the definition of a geochemical model (GM) for the clay-water system. The GM for a clay sample is defined in terms of relevant chemical processes taking place during aqueous extraction. Identification of GM requires knowing: 1) Aqueous complexes, 2) Mineral phases and their initial volume fractions and equilibrium constants, 3) Cation exchange reactions, cation exchange capacity (CEC) and cation selectivities, 4) Surface complexation reactions, types of sites, densities and protolysis constants, and 5) Gas phases, pressures and conditions (open or closed).

Since the appropriate GM may not be known *a priori*, it has to be improved in an iterative manner as indicated in Figure 1. The method starts from an initial GM and a guess of sample porewater concentrations, c_i. Inverse modelling accounts for the perturbations caused by aqueous extraction and computes concentrations of aqueous extracts. Optimum estimates of c_i are those which minimize the differences between measured and aqueous extracts concentrations. Large deviations of model results from measured data may indicate the need to modify or update the GM (see Figure 1).

2.3. Inverse model

Porewater chemistry is inferred with the inverse method of Dai and Samper (2004) which is based on generalized least squares. Let $\boldsymbol{p} = (p_1, p_2, p_3, \ldots, p_M)$ be the vector of M unknown parameters. The objective function, $E(\boldsymbol{p})$, can be expressed as

$$E(p) = \sum_{l=1}^{L_i} w_l^2 r_l^2 \tag{5}$$

where r_l is the residual of the lth data which is equal to the difference between computed and measured concentrations, w_l *is a* weighting coefficient for measured data and L_i is the number of dissolved species for which data are available. For FEBEX bentonite L_i is equal to 8 (see below). Weights, w_l, depend on data accuracy. If some data are judged unreliable, they should be assigned small weights in order to prevent their pernicious effect on optimization.

Inverse modelling of AET was performed with INVERSE-CORE^{2D} (Dai and Samper, 2004) a code which combines automatic parameter estimation algorithms with a reactive transport code CORE^{2D} (Samper *et al.*, 2003; Yang *et al.*, 2008). The inverse problem is solved by minimizing a generalized least-squares criterion with a Gauss-Newton-Levenberg-Marquardt method. CORE^{2D} and INVERSE-CORE^{2D} are finite element codes for modelling transient saturated and unsaturated water flow, heat transport and multicomponent reactive solute transport under both local chemical equilibrium and kinetic conditions. The chemical formulation is based on ion association theory and uses an extended version of Debye-Huckel equation (B-dot) for activity coefficients of aqueous species. CORE^{2D} and INVERSE-CORE^{2D} rely on thermodynamic data from EQ3/6 (Wolery, 1992). They have been used to interpret field experiments such as the Redox Zone Experiment in a fracture zone of the Äspö site (Molinero and Samper, 2004; Molinero *et al. 2*004; Molinero and Samper, 2006), analyze stochastic cation exchange reactive transport in aquifers (Samper and Yang, 2006), couple

chemical and biological processes within the context of the CERBERUS project in Boom clay (Samper *et al.* 2006; Zhang *et al.* 2008), evaluate interactions of bentonite-concrete (Yang *et al.*, 2007a), corrosion products and bentonite (Samper *et al.,* 2008c) and evaluate oxygen consumption in a HLW repository in granite (Yang *et al.,* 2007b). INVERSE-CORE^{2D} has been used to interpret laboratory experiments (Dai and Samper, 2004) and model geochemical processes in coastal systems (Dai and Samper, 2006; Dai *et al.* 2006).

3. Inverse analysis of AET data from FEBEX *in situ* test

3.1. Description of FEBEX in situ test

FEBEX (Full-scale Engineered Barrier EXperiment) is a demonstration and research project dealing with the bentonite engineered barrier designed for sealing and containment of a high-level radioactive waste repository (ENRESA, 2000). FEBEX is based on the Spanish reference concept for radioactive waste disposal in crystalline rock according to which canisters are emplaced in horizontal drifts and surrounded by a compacted bentonite clay barrier. The project includes two main large-scale tests which started in February 1997: a *mock-up* test operating at CIEMAT facilities in Madrid, Spain and an *in situ* full-scale test performed in a gallery excavated in granite at the Grimsel site, Switzerland (ENRESA, 2000). The gallery is 70.4 m long and has a diameter of 2.28 m. Two heaters were installed to maintain a maximum temperature of 100 ºC at the bentonite surface. A layout of the *in situ* test is shown in Fig. 2. Weighted averages of dry density and water content of bentonite blocks are 1.70 g/cm^3 and 14.4%, respectively (ENRESA, 2000). Mineralogical composition of FEBEX bentonite is listed in Table 1 (Fernández *et al.*, 2004). The main mineral phase (90-92 wt.%) is montmorillonite.

The FEBEX *in situ* test began in February 27th, 1997. Heater 1 was switched-off in 2002. A post-mortem bentonite sampling program was designed to characterize solid and liquid phases, measure physical and chemical changes induced by the combined effect of

heating and hydration; and to test model predictions (ENRESA, 2006a; Samper *et al.*, 2008a). Bentonite samples were taken from vertical sections normal to the axis of the tunnel (Fig.2). Fig. 3 shows the location of bentonite blocks in section 29 collected after dismantling of heater 1. A total of 9 bentonite blocks were sampled (BB29-5 to BB2913). Bentonite blocks were preserved immediately after their extraction in plastic films, two layers of aluminized PET-sheets and vacuum-sealed plastic bags. The first PET-sheet was vacuum sealed after flushing nitrogen in it. Protection against mechanical actions was used to ensure block integrity (Fernández and Rivas, 2003; ENRESA, 2006b). AET data from sections 29 and 19 located at both edges of heater 1 (see Fig. 2) were used to test our inverse methodology. Soluble salts of these two sections were analysed by Fernández and Rivas (2003) in aqueous extract solutions. Crushed bentonite samples were placed in contact with de-ionised and de-gassed water at a solid-to-liquid ratio of 1:4, shaken and allowed to react for 2 days at atmospheric conditions. After phase separation by centrifugation (30 min at 12.500 rpm), supernatant solutions were analysed.

3.2. Geochemical model

The geochemical model accounts for the following chemical processes: aqueous complexation, acid-base, mineral dissolution/precipitation, gas solution-exsolution, cation exchange and surface complexation. The chemical system is defined in terms of the following primary species: H_2O, H^+, Ca^{2+}, Mg^{2+}, Na^+, K^+, Cl^-, SO_4^{2-}, HCO_3^- and SiO_2(aq). Relevant aqueous complexes were identified from speciation runs performed with EQ3/6 (Wolery, 1992). They are listed in Table 2. Based on available hydrochemical data (Fernández *et al.*, 2004) relevant mineral phases for FEBEX bentonite include calcite, gypsum and chalcedony. Initial volume fraction of gypsum is assumed to be zero. For the duration of AET of 2 days these minerals can be assumed at chemical equilibrium. Dissolution of clays minerals such as

smectite is extremely slow and can be disregarded. The Gaines-Thomas convention is used for cation exchange.

Modelling of AET performed on bentonite samples of FEBEX *in situ* test assumes that all water content is accessible for chemical reactions. Chemical reactions used in the model and their corresponding equilibrium constants, selectivity coefficients and protolysis constants at 25 ºC are listed in Table 2.

Weights, w_l, in Equation 5 for inverse analysis are all equal to 1 except for bicarbonate data which are given a weight of 0.1 because initial bicarbonate concentrations are not estimated, but calculated from equilibrium with calcite. This is consistent with experimental conditions of FEBEX *in situ* test during which bentonite reacted with porewater for more than five years and reached equilibrium. Initial bicarbonate concentrations derived from equilibrium with calcite not always lead to a good fit to measured bicarbonate data. Adding bicarbonate data in the objective function does not help the estimation of initial bicarbonate. Actually, bicarbonate data affects the estimation of initial calcium concentration. In order to prevent the pernicious effect of bicarbonate data on the estimation of initial calcium concentration, bicarbonate data are given small weights.

As concluded by Fernández *et al.* (2004), protonation/deprotonation by surface sorption is a key process controlling pH and bentonite porewater chemistry. Previous studies have considered mostly a one-type of proton sorption sites (Wieland *et al.*, 1994). However, Bradbury and Baeyens (1997) argue that three types of proton adsorption sites are needed to describe titration data on SWy-1 montmorillonite and Ni/Zn sorption isotherms. Samper *et al.* (2008a) compared 1 and 3 types of proton sorption sites in a permeation test performed on a compacted sample of FEBEX bentonite. They conclude that protonation/deprotonation by surface sorption is a key process in buffering pH and that models with one and three types of proton sorption sites provide similar results. Therefore, here we use a model with a single type

of sorption site. Similar to Bradbury and Baeyens (1997) no electrical terms for surface complexation are considered.

Although our methodology accounts for redox reactions during water extraction, redox processes were not considered for the interpretation of AET performed on FEBEX bentonite because such processes are not relevant for the conditions of FEBEX *in situ* test. Bentonite samples from *in situ* test are at oxidizing conditions at which the redox processes most likely to occur are pyrite dissolution, organic matter oxidation, siderite dissolution and iron oxi-hydroxide dissolution/precipitation. FEBEX bentonite, however, has a very low content of organic matter, pyrite and siderite (see Table 1). Zheng *et al.* (2008) report the interpretation of AET performed on Opalinus clay samples by accounting for pyrite oxidation.

3.3 Model results

Inverse geochemical modelling has been performed for 9 samples of bentonite blocks in section 29 (Table 3) and 12 samples in section 19 (Table 4). Solution of the inverse problem provides optimum values of the initial concentrations which lead to calculated concentrations of the aqueous extract which for the most part reproduce measured concentrations.

Initial log *K* values of protolysis constants are equal to -5 for XOH_2^+ and 8.7 for XO^-. These protolysis constants lead to calculated pH much larger than measured pH (see Table 5). The fit to pH bicarbonate data is not good. The fit to measured pH and HCO_3^- data improves greatly when protolysis constants are also estimated in addition to initial concentrations. Estimated protolysis constants are equal to -5.8 for XOH_2^+ and 11.8 for XO^-. These estimates differ from initial estimates derived from Samper *et al.* (2008a) (see Table 5) probably

because they worked with compacted bentonite while here AET were performed on crushed bentonite.

Table 6 shows the inferred porewater chemical composition of a bentonite sample from section 19, BB19-14/5, with a water content 21.2%. The geochemical model reproduces most of the measured data except for pH and bicarbonate data.

In addition to dilution, dissolution/precipitation of minerals, cation exchange and surface complexation are the main geochemical processes that affect inferred porewater chemistry of FEBEX bentonite.

The effect of dilution on dissolved concentrations can be evaluated by means of Equation (4). In the absence of chemical reactions, the concentration of any species prior to aqueous extraction, c_i, can be computed from the concentration of aqueous extract, c_{ae}, by multiplying c_{ae} by the dilution factor in Equation 4. For reactive species, the initial concentration c_i differs from Fc_{ae} due to chemical sink/sources which may be evaluated by comparing Fc_{ae} with the inverse-estimate c_i. Figure 4 shows the comparison of c_{ae} (measured aqueous extract), Fc_{ae} (pure dilution) and c_i (inferred) concentrations for dissolved calcium. One can see that pure dilution concentrations (Fc_{ae}) are much larger than measured concentrations (c_{ae}). They differ by a factor F which for samples in section 29 range from 20 to 33 (see Table 3). Inferred concentrations, c_i, are larger than pure dilution concentrations by at least a factor of 5 (see Figure 4). This means that the net effect of chemical reactions is a sink for dissolved calcium. Calcite dissolution provides a source of calcium while cation exchange acts as a sink for dissolved calcium. When these two processes are combined, they lead to a net sink of calcium, indicating that cation exchange plays a more important role in controlling the final concentration of calcium than calcite dissolution. Results for dissolved magnesium (Fig. 5) are similar to those of calcium and reflect that dissolved magnesium is exchanged with sorbed cations.

Dissolved sodium (Fig. 6) and potassium (Fig. 7) have sources coming from cation exchange since their inferred values are smaller than those calculated from pure dilution. Since the initial volume fraction of gypsum is zero, gypsum does not precipitate during aqueous extract and dissolved sulphate behaves as a conservative species (Fig. 8). As a result, inferred sulphate concentrations coincide with sulphate calculated from pure dilution. Model results for bicarbonate indicate that there is a source due to calcite dissolution so that inferred concentrations (Fig. 9) are smaller than those calculated from pure dilution.

Inferred concentrations of chemical species for bentonite samples of sections 29 and 19 are listed in Tables 7 and 8. Samper *et al.* (2008a) present a discussion of the interpretation of the chemical composition of FEBEX *in situ* test after heating and hydration processes.

Calcite dissolution in aqueous extract tends to increase pH. However, surface complexation reactions buffer pH. Therefore, most inferred pH values are slightly smaller than measured aqueous extract pH (Fig. 10). The maximum difference between measured and inferred pH is less than 0.3. The spatial distribution of inferred pH does not show a clear trend due to pH buffering processes.

4. Uncertainties

Our inverse hydrochemical model to interpret AET has uncertainties related to: 1) Initial amount of soluble minerals; 2) Relevant mechanism for mineral dissolution/precipitation (kinetics versus equilibrium); 3) Types of sorption sites and 4) Relevance of pH-buffering processes.

4.1 Initial amount of gypsum

According to ENRESA (2000), FEBEX bentonite at ambient conditions (water content of about 14%) contains 0.14 wt% of gypsum (0.08% in volume fraction) (see Table 1). Bentonite samples from *in situ* test were subjected simultaneously to heating and hydration. During the test gypsum could have been dissolved due to hydration or precipitated near the heater due to

evaporation. No mineralogical characterizations were performed before AET and therefore the initial amount of gypsum before AET is unknown. This is a source of uncertainty in AET interpretation. Whenever present, gypsum controls dissolved sulphate concentrations. Thereby, the saturation index with respect to gypsum provides a hint on the presence of gypsum. Aqueous extracts from sections 29 and 19 are markedly undersaturated with respect to gypsum (see Tables 3 and 4). Since samples are diluted during extraction, original bentonite porewater could be less unsaturated than aqueous extracts.

Saturation indexes were calculated also with concentrations of initial water (chemical composition before aqueous extract) by assuming pure dilution for all species. After accounting for dilution, most samples are still undersaturated with respect to gypsum although some samples are close to saturation. All these calculations indicate that bentonite samples most likely do not contain gypsum.

A sensitivity run was conducted to test the effect of assuming an initial amount of gypsum. The inverse model was run for BB29-11/2-3 by assuming an initial volume fraction of gypsum equal to that reported in ENRESA (2000) for intact bentonite which is equal to 0.08%. Model results for this sensitivity run are compared to those of the base run in Table 9. It can be seen that the inverse model with an initial amount of gypsum fails to fit measured sulphate and calcium data. Inverse estimate (inferred) of sulphate concentration is smaller than that of the base run. Therefore, it can be concluded that most bentonite samples from FEBEX in situ test do not contain gypsum.

4.2 Kinetic dissolution of calcite

According to Samper *et al.* (2005), dissolved HCO_3^- and Ca^{2+} concentrations are slightly affected by kinetic calcite dissolution. Aqueous extracts after 2 days may have not reached equilibrium and therefore measured dissolved concentrations may be smaller than those predicted with an equilibrium model.

Aqueous extracts from section 29 are all slightly undersaturated with respect to calcite (see Table 3), Therefore after 2 days of aqueous extraction, samples have not reached equilibrium with respect to calcite because its dissolution is kinetically controlled**.**

On the other hand, porewaters in bentonite samples from FEBEX *in situ* test have been in contact with mineral phases for more than 5 years and therefore are likely to be at equilibrium with calcite. Therefore, the interpretation of AET must to take into account two distinct conditions: (1) Initial porewater in bentonite samples is likely to be at equilibrium with calcite; (2) Kinetic calcite dissolution takes place during AET, leading to undersaturated aqueous extract samples. Here arises the question of how to estimate the initial porewater composition which is at equilibrium from measured AET data which are not at equilibrium with respect to calcite. Since the computer code we used to interpret AET cannot handle this type of problem, it was decided to assume calcite equilibrium both initially and during aqueous extraction. This deviation from reality leads to problems in fitting bicarbonate data. Future studies should improve the interpretation of AET for FEBEX bentonite by allowing for initial equilibrium conditions and transient kinetic mineral dissolution during extraction.

4.3 Types of surface complexation sites

Samper *et al.* (2008a) compared 1 and 3 types of proton sorption sites in a permeation test performed on a compacted sample of FEBEX bentonite. They report that protonation/deprotonation by surface sorption is a key process in buffering pH and that models with one and three types of proton sorption sites provide similar results. Here we compare models with 1 and 3 types of sorption sites while keeping constant the total concentration of sorption sites. Model results are similar in both cases, although there are small differences in pH (see Table 5).

4.4 pH buffering processes

Sensitivity analyses performed by Zheng (2006) on a coupled THMC model of the FEBEX *in situ* test indicate that surface complexation is more relevant than calcite dissolution in buffering pH. In order to evaluate the relevance of different pH buffering processes, several sensitivity runs were performed with sample BB29-11/2-3. Initial concentrations for sensitivity runs are equal to those inferred for sample BB29-11/2-3 (see Table 5). In the first sensitivity run, surface complexation is taken out. In this case pH is buffered by calcite dissolution and CO_2 dissolution. In the absence of surface complexation, calcite dissolution induces a noticeable increase in pH. In the second sensitivity run, both surface complexation and calcite dissolution are dropped. As a result, CO_2 dissolution causes a decrease in pH. In the absence of calcite, calculated calcium is smaller than in previous cases (Table 10). Therefore, it can be concluded also that surface complexation is more relevant than calcite dissolution in buffering pH.

4.5 Other uncertainties

Our model for the interpretation of AET of bentonite samples fails to fit bicarbonate and pH data probably due to the fact that the model assumes a fixed pressure of CO_2(g) during aqueous extraction. Such deviations may be overcome by using a variable CO_2 gas pressure. Although the inverse model of FEBEX bentonite aqueous extracts assumes that all water content is accessible for chemical reactions, the inverse method can deal with accessible porosity smaller than total porosity and with more complex porosity structures (Samper *et al.* 2008b).

Our inverse method estimates pH and concentrations of original clay sample without checking for charge balance. Charge balance errors are less than 10% if surface complexes XOH_2^+ and XO^- are considered in the charge balance calculation. Concentrations of XOH_2^+ in

FEBEX samples are 3 orders of magnitude larger than those of XO^-. They are on the order of 10^{-1} mol/L and compensate for the lack of positive charges. The inverse methodology should be extended to ensure charge neutrality of estimated chemical composition of clay samples.

5. Conclusions

A numerical methodology for quantitative interpretation of aqueous extract tests has been presented. Contrary to squeezing which is only feasible for samples with large water content, aqueous extraction can be used for samples of any water content. Numerically-interpreted aqueous extract tests, AET, not only provide an efficient alternative to squeezing, but also offer a robust, flexible and comprehensive way to estimate the original chemical composition of clay porewater from measured mineralogy, water content and composition of extract water. The inverse problem has been solved with INVERSE-CORE^{2D}. Inverse interpretation of AET has been shown to work well for bentonite samples taken from FEBEX *in situ* test. Zheng *et al.* (2008) report its application samples of Opalinus clay from a ventilation experiment.

The inverse method to interpret AET provides a comprehensive way to estimate the chemical composition of clay porewater because it accounts for a wide range of chemical processes such as acid-base, redox, aqueous complexation, mineral dissolution/precipitation, gas dissolution/ex-solution, cation exchange and surface complexation. It provides also the flexibility to account for tests performed with different *S/L* ratios. For gaseous species, the chemical system can be treated either as open with prescribed gas pressures or closed.

Acknowledgments

This work has been performed within the framework of FEBEX project funded by ENRESA and the European Union through contracts FI4W-CT95-0006 and FIKW-CT-2000-00016 of the Nuclear Fission Program. This manuscript was also partially funded through Contract No.

DE-AC02-05CH11231 with the U.S. Department of Energy. We thank the University of La Coruña for the research scholarship awarded to the first author. Contributions of UDC researchers who participated throughout the various stages of the FEBEX project are acknowledged. Thanks are given to the two anonymous reviewers for constructive and enriching comments, suggestions and recommendations which contributed to the improvement of the paper.

References

Alonso, E.E., Ledesma, A. (Eds.), 2005. Advances in Understanding Engineered Clay Barriers. A.A. Balkema Publishers, Leiden, The Netherlands.

Arcos, D., Bruno, J., Karnland, O., 2003. Geochemical model of the granite-bentonite-groundwater interaction at Äspö HRL (LOT experiment). Appl. Clay Science 23, 219-228.

Beaucaire, C., Pitsch, H., Toulhoat, P., Motellier, S., Louvat, D., 2000. Regional fluid characterisation and modelling of water-rock equilibria in the Boom clay formation and in the Rupelian aquifer at Mol, Belgium. Appl. Geochem. 15, 667-686.

Bradbury, M.H., Baeyens, B., 1997. A mechanistic description of Ni and Zn sorption on Na-montmorillonite. Part II: Modelling. J. Contam. Hydrol. 27, 223-248.

Bradbury, M.H., Baeyens, B., 1998. A physicochemical characterisation and geochemical modelling approach for determining porewater chemistries in argillaceous rocks. Geochim. Cosmochim. Acta 62, 783-795.

Bradbury, M.H., Baeyens, B., 2003. Porewater chemistry in compacted resaturated MX-80 bentonite. J. Contam. Hydrol. 61, 329-338.

Cuevas, J., Villar, M.V., Fernández, A.M., Gómez, P., Martín, P.L., 1997. Pore waters extracted from compacted bentonite subjected to simultaneous heating and hydration. Appl. Geochem. 12, 473-481.

Dai Z., Samper, J., 2004. Inverse problem of multicomponent reactive chemical transport in porous media: Formulation and Applications. Water Resources Research, Vol. 40, W07407, doi:10.1029/2004WR003248.

Dai Z., Samper, J., 2006. Inverse modeling of water flow and multicomponent reactive transport in coastal aquifer systems. J. of Hydrol. 327, Issues 3-4, 447-461.

Dai Z., Samper J., Ritzi, R., 2006. Identifying geochemical processes by inverse modeling of multicomponent reactive transport in Aquia aquifer, Geosphere, Vol. 4, Nº 4, 210–219.

ENRESA, 2000. Full-scale engineered barriers experiment for a deep geological repository in crystalline host rock (FEBEX Project). European Commission. EUR 19147 EN.

ENRESA, 2006a. FEBEX: Updated final report. ENRESA Techn. Publ. PT 05-0/2006, 589 pp.

ENRESA, 2006b. FEBEX: Post-mortem bentonite analysis. ENRESA Techn. Publ. PT 05-1/2006, 183 pp.

Fernández, A.M., Rivas, P., 2003. Task 141: Post-mortem bentonite analysis. Geochemical behaviour. CIEMAT Internal Note 70-IMA-L-0-107 v0.

Fernández, A.M., Baeyens, B., Bradbury, M., Rivas, P., 2004. Analysis of the pore water chemical composition of a Spanish compacted bentonite used in an engineered barrier. Physics and Chemistry of the Earth 29(1), 105-118.

Fritz, B., Kam, M., 1985. Chemical interactions between the bentonite and the natural solutions from the granite near a repository for spent nuclear fuel. SKB Technical Report TR-85-10.

Gaucher, E.C., Blanc, P., Bardot, F., Braibant, G., Buschaert, S., Crouzet, C., Gautier, A., Girard, J.P., Jacquot, E., Lassin, A., Negrel, G., Tournassat, C., Vinsot, A., Altmann, S., 2006. Modelling the porewater chemistry of the Callovian–Oxfordian formation at a regional scale. Comptes Rendus Geosciences 338, 917-930.

Kraepiel, A.M.L., Keller, K., Morel, F.M.M., 1998. On the acid-base chemistry of permanently charged minerals. Environ. Sci. Technol. 32, 2829-2838.

Metz, V., Kienzler, B., Schüβler, W., 2003. Geochemical evaluation of different groundwater-host rock systems for radioactive waste disposal. J. Cont. Hydrol. 61, 265–279

Molinero J., Samper, J., 2004. Groundwater flow and solute transport in fracture zones: An improved model for a large-scale field experiment at Äspö (Sweden). J. Hydraulic Research. 42, 157-172.

Molinero, J., Samper, J., 2006. Modeling of reactive solute transport in fracture zones of granitic bedrocks. J. Cont. Hydrol. 82, 293–318.

Molinero, J., Samper, J., Yang, C., Zhang, G., 2004. Biogeochemical reactive transport model of the Redox zone experiment of the Äspö hard rock laboratory (Sweden). Nuclear Technology 48(2), 151-165.

Muurinen, A., Lehikoinen, J., 1999. Pore water chemistry in compacted bentonite. Engineering Geology 54, 207-214.

Muurinen, A., Karnland, O., Lehikoinen, J., 2004. Ion concentration caused by an external solution into the porewater of compacted bentonite. Physics and Chemistry of the Earth 29, 119-127.

Ochs, M., Lothenbach, B., Shibata, M., Yui, M., 2004. Thermodynamic modelling and sensitivity analysis of porewater chemistry in compacted bentonite. Physics and Chemistry of the Earth 29, 129-136

Parshiva-Murthy, A.S., Ferrel, R.E. Jr., 1972. Comparative chemical composition of sediments interstitial waters. Clay and Clay Min. 20, 317-321.

Parshiva-Murthy, A.S., Ferrel, R.E. Jr., 1973. Distribution of major cations in esturarine sediments. Clay and Clay Min. 21, 161-165.

Pearson, F.J., Arcos, D., Bath, A., Boisson, J.-Y., Fernández, A.M., Gäbler, H.-E., Gaucher, E., Gautschi, A., Griffault, L., Hernán, P., Waber, H.N., 2003. Mont Terri Project - Geochemistry of water in the Opalinus Clay Formation at the Mont Terri Rock Laboratory. Swiss Federal Office for Water and Geology Series Nº 5. Bern.

Sacchi, E., Michelot, J.L., Pitsch, H., Lalieux, P., Aranyossy, J.F., 2001. Extraction of water and solutes from argillaceous rocks for geochemical characterization: Methods, processes, and current understanding. Hydrogeology Journal 9, 17-33.

Samper J., Yang, C., 2006, Stochastic Analysis of Transport and Multicomponent Competitive Monovalent Cation Exchange in Aquifers, Geosphere, Vol. 2, 102-112.

Samper, J., Yang, C., Montenegro, L., 2003. Users Manual of CORE^{2D} version 4: A COde for groundwater flow and REactive solute transport. University of A Coruña, Spain.

Samper, J., Vázquez, A., Montenegro, L., 2005. Inverse hydrochemical modelling of aqueous extracts experiments for the estimation of FEBEX bentonite pore water chemistry. In: Alonso, E.E., Ledesma, A. (Eds.), Advances in Understanding Engineered Clay Barriers. A.A. Balkema Publishers, Leiden, The Netherlands, 553-563.

Samper, J., Zhang, G., Montenegro, L., 2006. Coupled microbial and geochemical reactive transport models in porous media: Formulation and Application to Synthetic and *In situ* Experiments. Journal of Iberian Geology 32(2), 211-217.

Samper, J., Zheng, L., Montenegro, L., Fernández, A.M., Rivas, P., 2008a. Testing coupled thermo-hydro-chemical models of compacted bentonite after dismantling the FEBEX *in situ* test. Appl. Geochem. (in press).

Samper, J., Zheng, L., Fernández, A.M., Montenegro, L., 2008b. Inverse modelling of multicomponent reactive transport through single and dual porosity media. J. Cont. Hydrol. (accepted).

Samper, J., Lu, C., Montenegro, L., 2008c. Coupled hydrogeochemical calculations of the interactions of corrosion products and bentonite. Physics and Chemistry of the Earth (accepted).

Sasamoto, H., Yui, M., Arthur, R.C., 2007. Estimation of *in situ* groundwater chemistry using geochemical modelling: A test case for saline type groundwater in argillaceous rock. Physics and Chemistry of the Earth 32, 196-208.

Turrero, M.J., Fernández, A.M., Peña, J., Sánchez, M.D., Wersin, P., Bossart, P., Sánchez, M., Melón, A., Garralón, A., Yllera, A., Gómez, P., Hernán, P., 2006. Pore water chemistry of a Palogene continental mudrock in Spain and a Jurassic marine mudrock in Switzerland: Sampling methods and geochemical interpretation. Journal of Iberian Geology 32(2), 233-258.

Wanner, H., Albinsson, Y., Karnland, O., Wieland, E., Wersin, P., Charlet, L., 1994. The acid/base chemistry of montmorillonite. Radiochim. Acta 66/67, 157-162.

Wieland, E., Wanner, H., Albinsson, Y., Wersin, P., Karnland, O., 1994. A surface chemical model of the bentonite-water interface and its implications for modelling the near field chemistry in a repository for spent fuel. SKB Technical Report TR-94-26, Stockholm, Sweden.

Wersin, P., 2003. Geochemical modelling of bentonite porewater in high-level waste repositories. J. Contam. Hydrol. 61, 405-422.

Wersin, P., Curti, E., Appelo, C.A.J., 2004. Modelling bentonite-water interactions at high solid/liquid ratios: swelling and diffusive double layer effects. Applied Clay Science 26, 249-257.

Wolery, T.J., 1992. EQ3/6, a software package for geochemical modeling of aqueous systems: Package overview and installation guide (version 7.0). Technical Report UCRL-MA-110662-Pt 1. Lawrence Livermore National Laboratory, CA, USA.

Yang, C., Samper, J., Montenegro, L. 2007a. A coupled non-isothermal reactive transport model for long-term geochemical evolution of a HLW repository in clay. Environ. Geol., DOI 10.1007/s00254-007-0770-2.

Yang, C., Samper, J., Molinero J., Bonilla, M., 2007b. Modelling geochemical and microbial consumption of dissolved oxygen after backfilling a high level radiactive waste repository. J. Contam. Hydrol. 93, 130-148.

Yang, C., Samper, J., Montenegro, L., 2008. CORE V4: A general purpose code for groundwater flow, heat and solute transport, chemical reactions and biological processes in porous and fractured media. Physics and Chemistry of the Earth (submitted).

Zhang, G., Samper, J., Montenegro L., 2008. Coupled thermo-hydro-bio-geochemical reactive transport model of the CERBERUS heating and radiation experiment in Boom clay. Appl. Geochem. doi:10.1016/j.apgeochem.2007.09.010.

Zheng, L., Samper, J., Montenegro L., Mayor, J.C., 2008. Flow and reactive transport model of a ventilation experiment in Opallinus clay. Physics and Chemistry of the Earth (submitted).

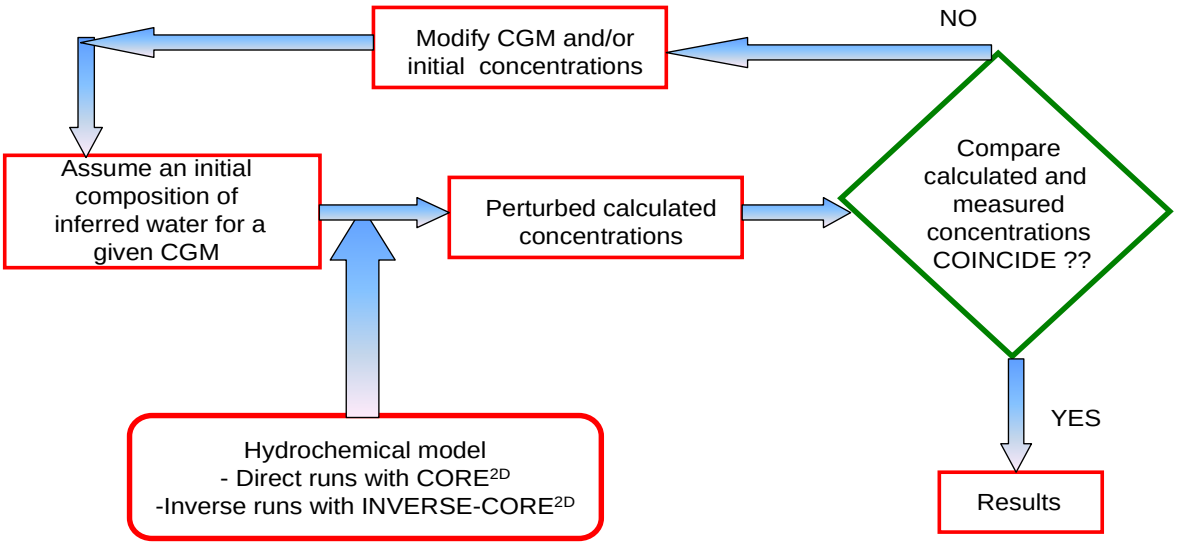

Fig. 1. Flowchart of the methodology for inverse estimation of initial chemical composition of clay sample from measured aqueous extract data.

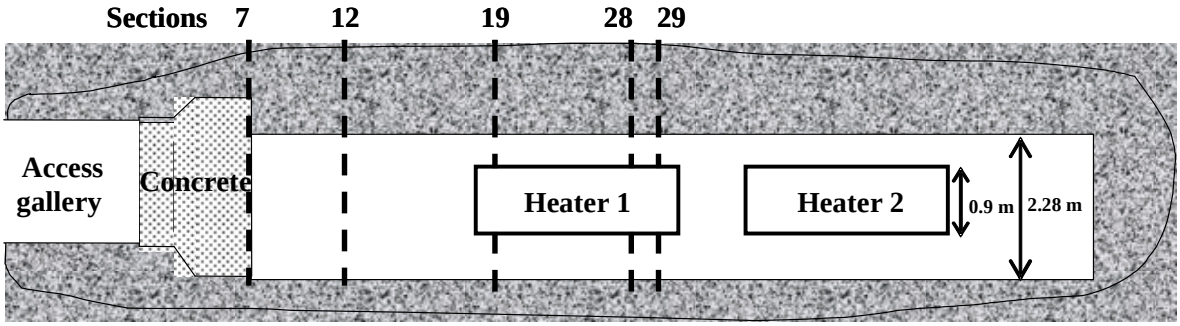

Fig. 2. Layout of FEBEX *in situ* test. Vertical lines show the location of the different sampling sections.

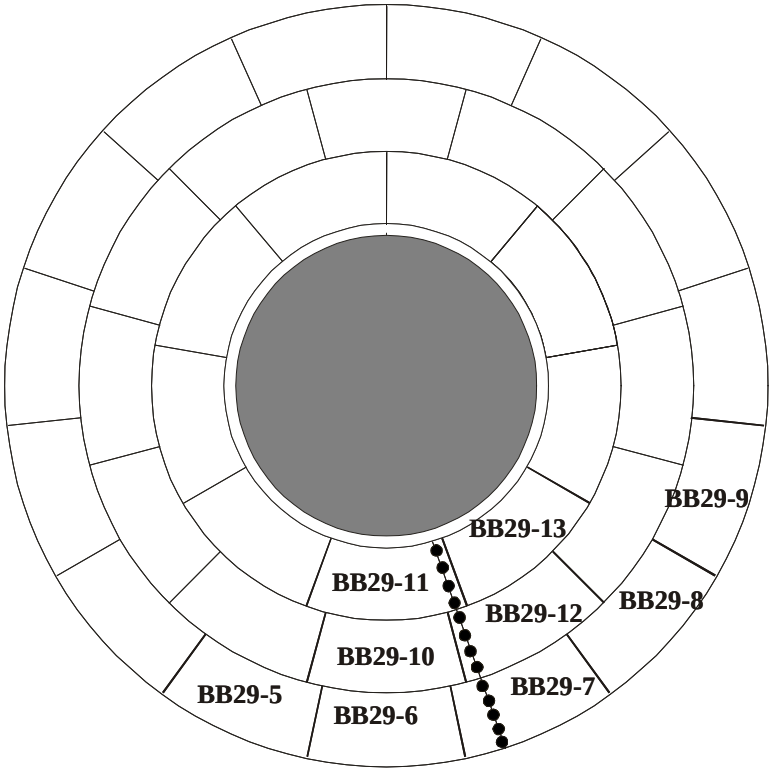

Fig. 3. Location of bentonite blocks (BB29-5 to BB-29-13) in sampling section 29 collected after dismantling of heater 1 of FEBEX *in situ* test.

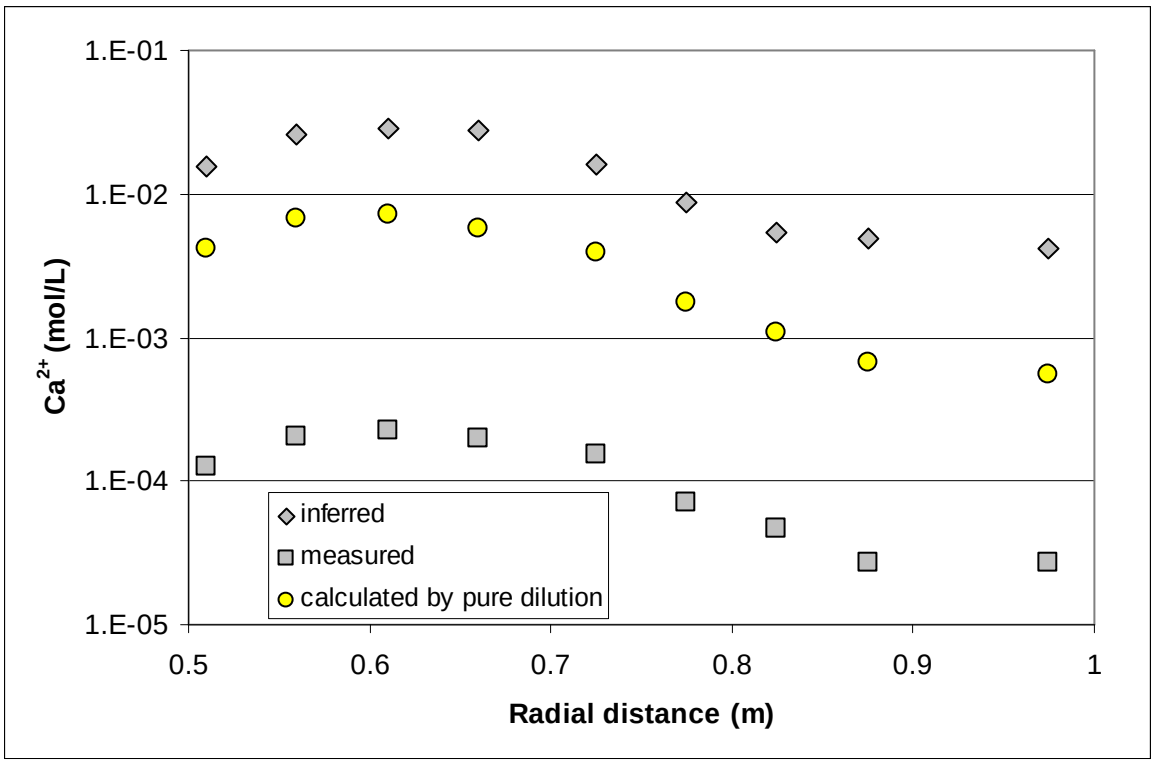

Fig. 4. Comparison of measured aqueous extract concentrations, $c_{ae,}$ with those calculated by pure dilution (Fc_a) for dissolved calcium in section 29. Inverse estimate of initial concentrations (inferred) are larger than pure dilution concentrations meaning that there is a net sink of dissolved calcium.

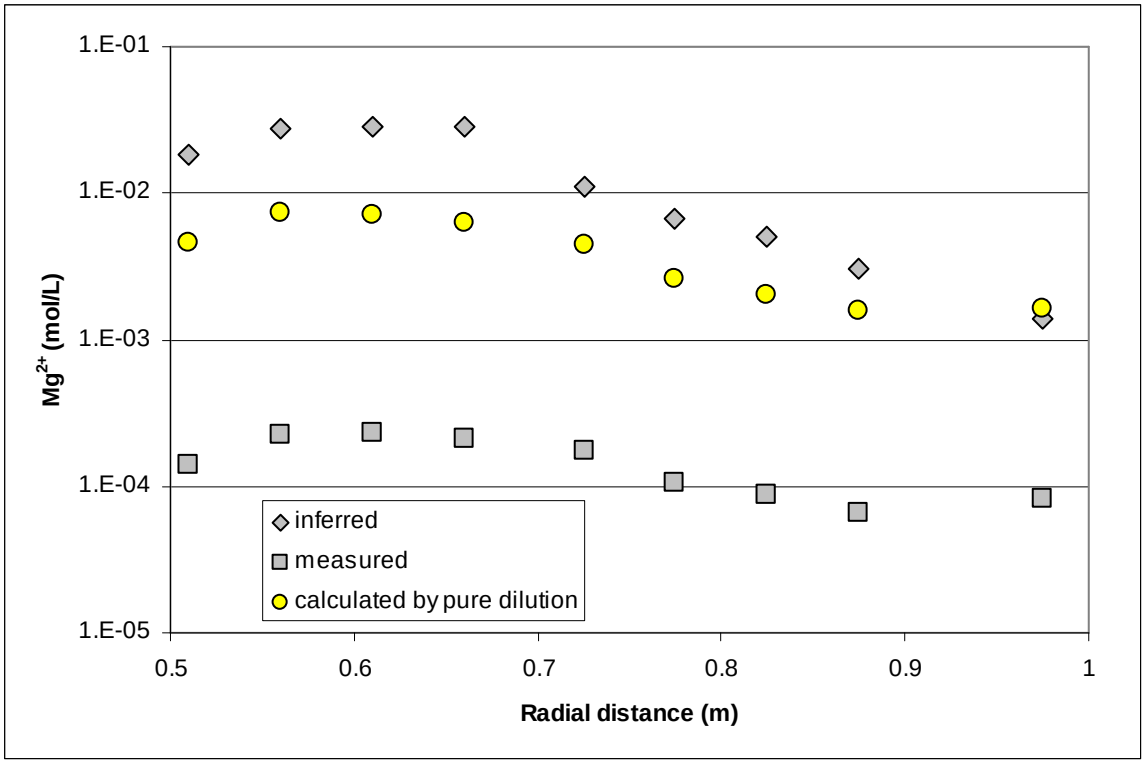

Fig. 5. Comparison of measured aqueous extract concentrations, $c_{ae,}$ with those calculated by pure dilution (Fc_a) for dissolved magnesium in section 29. Inverse estimate of initial concentrations (inferred) are larger than pure dilution concentrations meaning that there is a net sink of dissolved magnesium due to cation exchange.

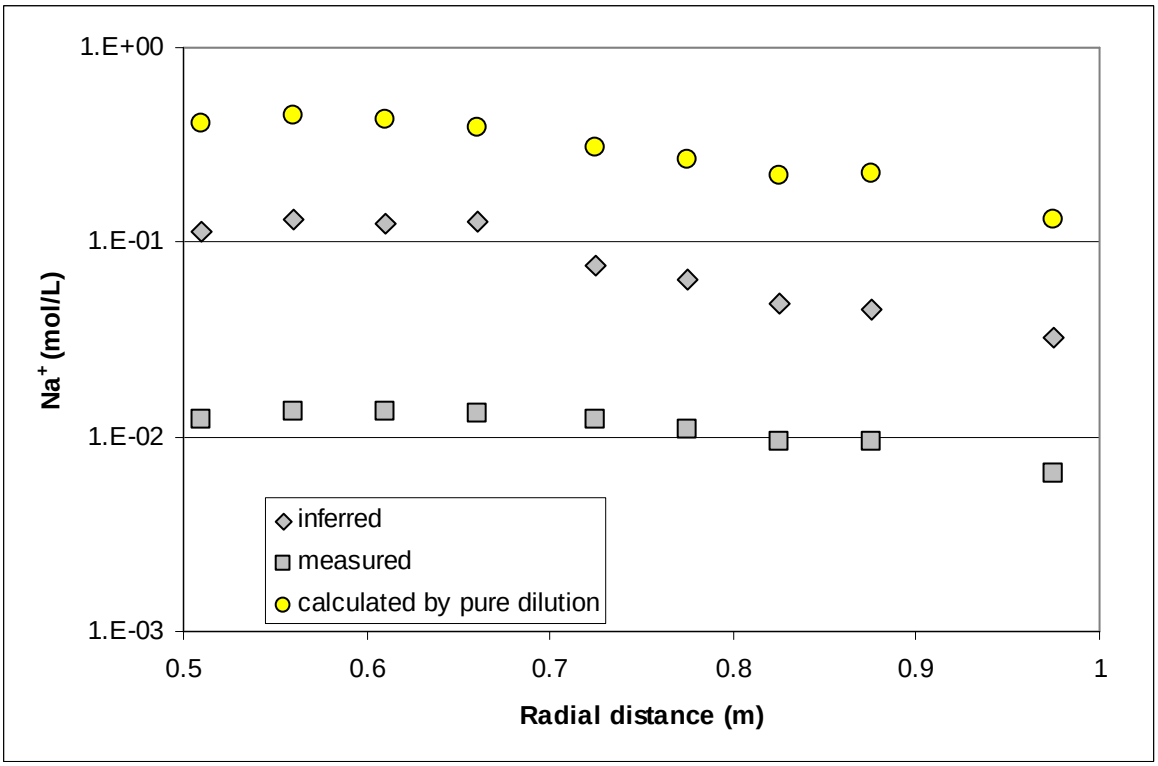

Fig. 6. Comparison of measured aqueous extract concentrations, $c_{ae,}$ with those calculated by pure dilution (Fc_a) for dissolved sodium in section 29. Inverse estimate of initial concentrations (inferred) are smaller than pure dilution concentrations meaning that there is a net source of dissolved sodium due to cation exchange.

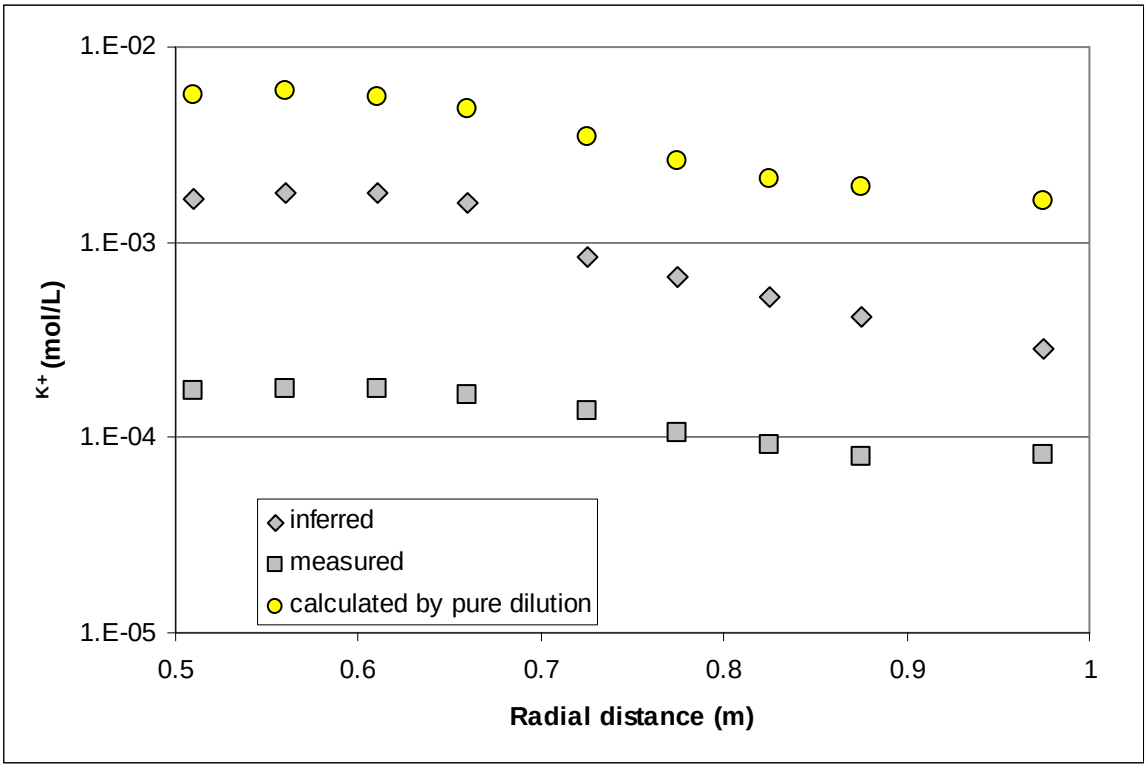

Fig. 7. Comparison of measured aqueous extract concentrations, $c_{ae,}$ with those calculated by pure dilution (Fc_a) for dissolved potassium in section 29. Inverse estimate of initial concentrations (inferred) are smaller than pure dilution concentrations meaning that there is a net source of dissolved potassium due to cation exchange.

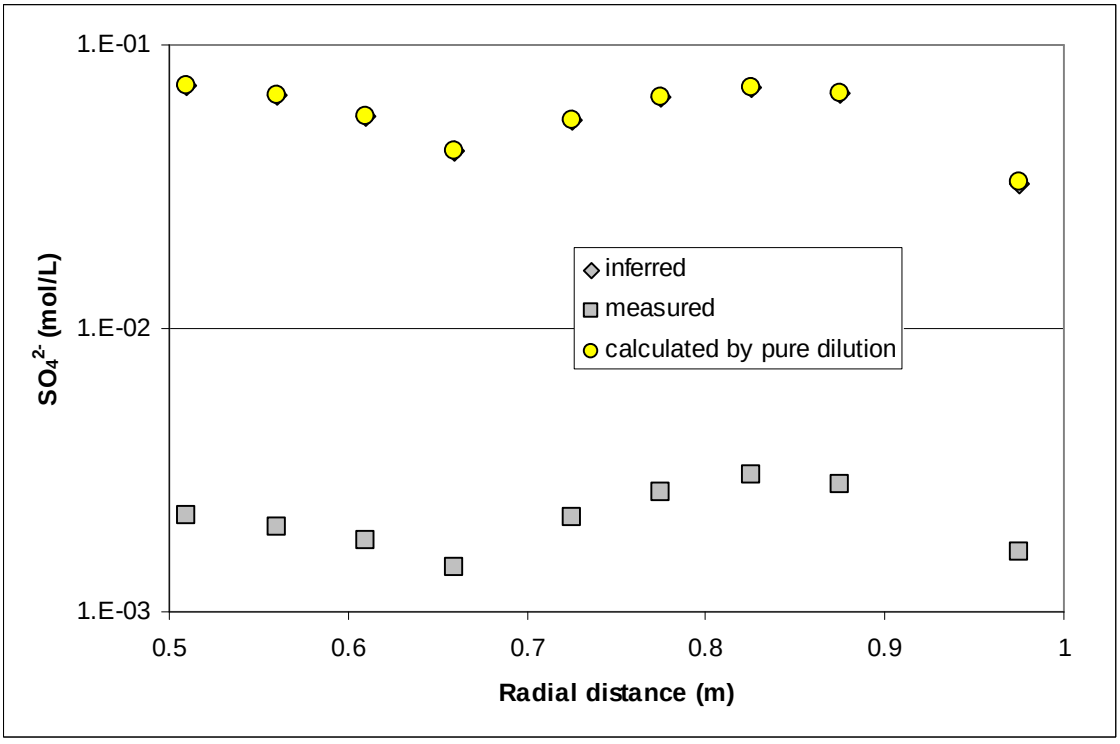

Fig. 8. Comparison of measured aqueous extract concentrations, $c_{ae,}$ with those calculated by pure dilution (Fc_a) for dissolved sulphate in section 29. Inverse estimate of initial concentrations (inferred) coincide with pure dilution concentrations because in this case sulphate behaves as a conservative species.

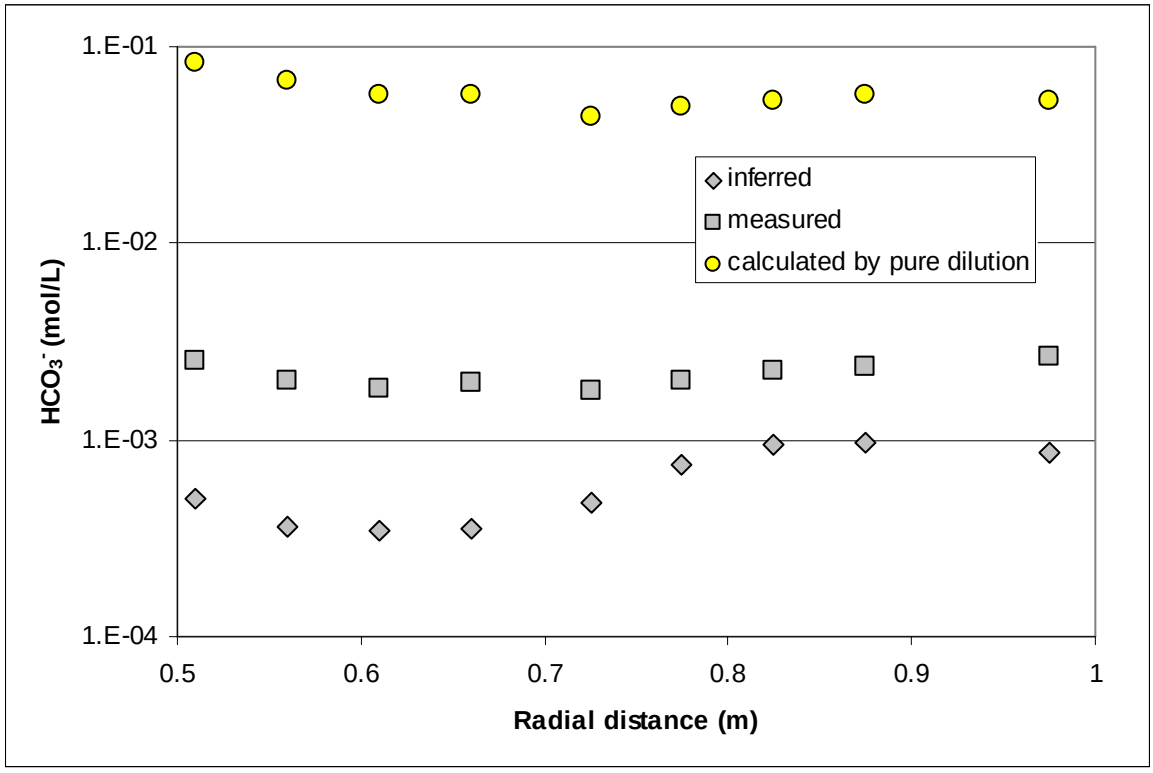

Fig. 9. Comparison of measured aqueous extract concentrations, $c_{ae,}$ with those calculated by pure dilution (Fc_a) for dissolved bicarbonate in section 29. Inverse estimate of initial concentrations (inferred) are much smaller than pure dilution concentrations meaning that there is a net source of dissolved bicarbonate due to calcite dissolution.

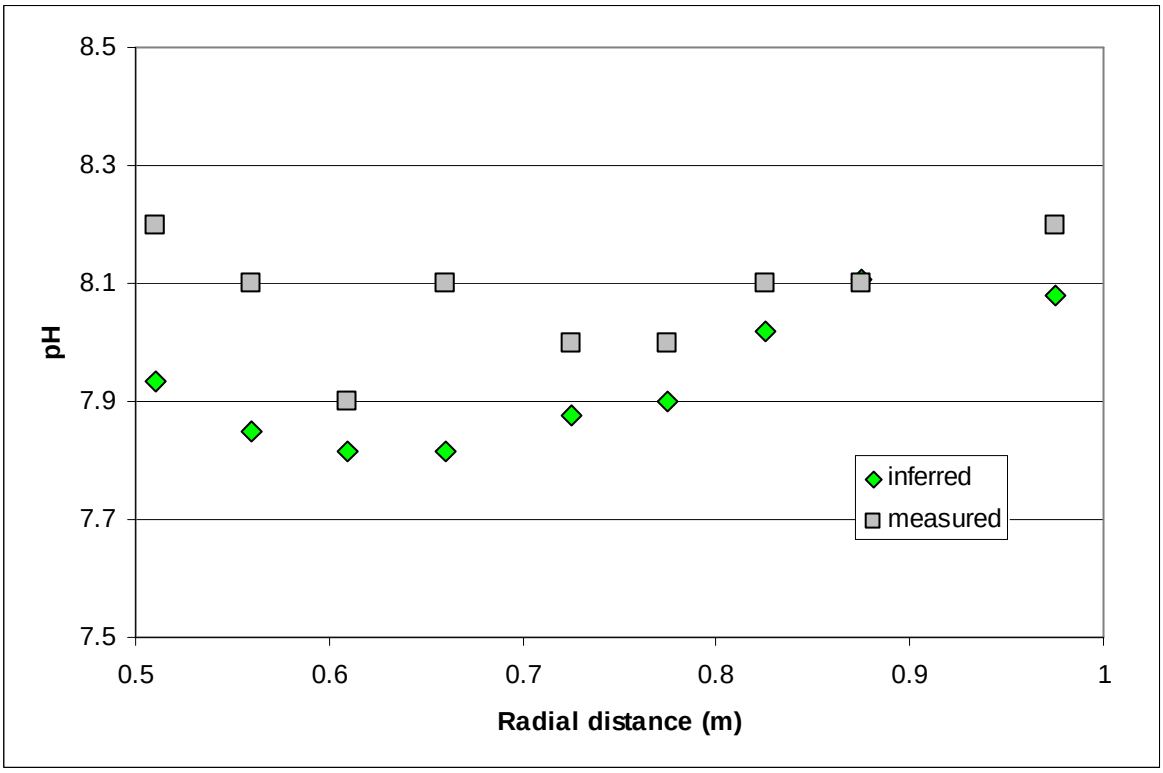

Fig. 10. Comparison of measured aqueous extract pH and inverse estimate of initial pH (inferred) at section 29.

Table 1. Mineralogical composition (in weight %) of FEBEX bentonite (Fernández *et al.*, 2004).

Main minerals		Accessory minerals		Poorly ordered minerals	
Smectite	92 ± 3	Organic Matter (as CO_2)	0.35 ± 0.05	SiO_2	0.038 ± 0.005
Quartz	2 ± 1	Carbonates (calcite, dolomite)	0.60 ± 0.13		
Plagioclase	2 ± 1	Soluble sulfates (gypsum)	0.14 ± 0.01	Al_2O_3	0.035 ± 0.005
Cristobalite	2 ± 1	Less soluble sulfates (barite, celestite)	0.02 ± 0.00		

Table 2. Equilibrium constants for aqueous complexes, minerals and gases, selectivity coefficients for cation exchange reactions; and protolysis constants for surface complexation reactions.

Aqueous complexes	Log K (25 ºC)
$CaCl^+ \Leftrightarrow Ca^{2+} + Cl^-$	0.70457
$CaCO_3(aq) + H^+ \Leftrightarrow Ca^{2+} + HCO_3^-$	7.1009
$CaHCO_3^+ \Leftrightarrow Ca^{2+} + HCO_3^-$	-1.04111
$CaSO_4(aq) \Leftrightarrow Ca^{2+} + SO_4^{2-}$	-2.0855
$CO_2(aq) + H_2O \Leftrightarrow H^+ + HCO_3^-$	-6.3733
$CO_3^{2-} + H^+ \Leftrightarrow HCO_3^-$	10.371
$H_2SiO_4^{2-} + 2\ H^+ \Leftrightarrow 2\ H_2O + SiO_2(aq)$	22.9116
$HSiO_3^- + H^+ \Leftrightarrow H_2O + SiO_2(aq)$	9.9525
$KSO_4^- \Leftrightarrow K^+ + SO_4^{2-}$	-0.86822
$MgCl^+ \Leftrightarrow Mg^{2+} + Cl^-$	0.13413
$MgCO_3(aq) \Leftrightarrow Mg^{2+} + CO_3^{-2}$	-7.428
$MgHCO_3^+ \Leftrightarrow Mg^{2+} + HCO_3^-$	-1.0295
$MgSO_4(aq) \Leftrightarrow Mg^{2+} + SO_4^{2-}$	-2.3228
$NaHCO_3(aq) \Leftrightarrow Na^+ + HCO_3^-$	-0.2118
$NaSO_4^- \Leftrightarrow Na^+ + SO_4^{2-}$	-0.79855
$OH^- + H^+ \Leftrightarrow H_2O$	14.16
Minerals	Log K (25 ºC)
$CaCO_3(s) + H^+ \Leftrightarrow Ca^{2+} + HCO_3^-$	1.9299
$CaSO_4(s) \Leftrightarrow Ca^{2+} + SO_4^{2-}$	-4.2451
$CaSO_4 \cdot 2H_2O(s) \Leftrightarrow Ca^{2+} + SO_4^{2-} + 2H_2O$	-4.4699
$SiO_2(s) \Leftrightarrow SiO_2(aq)$	-3.8334
Gases	Log K (25 ºC)
$CO_2(g) + H_2O \Leftrightarrow H^+ + HCO_3^-$	-7.8136
Cation exchange	$K_{Na\text{-}cation}$
$Na^+ + X\text{-}K \Leftrightarrow K^+ + X\text{-}Na$	0.138
$Na^+ + 0.5X_2\text{-}Ca \Leftrightarrow 0.5Ca^{2+} + X\text{-}Na$	0.2942
$Na^+ + 0.5Mg\text{-}X_2 \Leftrightarrow 0.5Mg^{2+} + Na\text{-}X$	0.2881
Surface complexation	Log K_{int}
$XOH_2^+ \Leftrightarrow XOH + H^+$	-5.8
$XO^- + H^+ \Leftrightarrow XOH$	11.8

Table 3. Chemical composition (in mol/L) of 1:4 aqueous extracts from bentonite samples at different radial distances along section 29. Also listed are dilution factors, *F*, defined in Equation 4 and saturation indexes with respect to calcite and gypsum.

Sample	Radial distance (cm)	w.c. (%)	Dilution factor	pH	HCO_3^-	SO_4^{2-}	Cl^-	K^+	Na^+	Mg^{2+}	Ca^{2+}	SI calcite	SI Gypsum
BB29-7/1-10	97.5	26.5	20.09	8.2	$2.7\cdot10^{-3}$	$1.6\cdot10^{-3}$	$8.2\cdot10^{-4}$	8.210^{-5}	$6.4\cdot10^{-3}$	$8.2\cdot10^{-5}$	$2.7\cdot10^{-5}$	-0.87	-3.85
BB29-12/2-1	87.5	21	24.05	8.1	$2.3\cdot10^{-3}$	$2.8\cdot10^{-3}$	$1.7\cdot10^{-3}$	7.910^{-5}	$9.4\cdot10^{-3}$	$6.6\cdot10^{-5}$	$2.7\cdot10^{-5}$	-1.02	-3.61
BB29-12/2-2	82.5	22	23.18	8.1	$2.3\cdot10^{-3}$	$3.1\cdot10^{-3}$	$2.1\cdot10^{-3}$	9.210^{-5}	$9.5\cdot10^{-3}$	$8.6\cdot10^{-5}$	$4.7\cdot10^{-5}$	-0.80	-3.34
BB29-12/2-3	77.5	20.3	24.70	8	$2.0\cdot10^{-3}$	$2.7\cdot10^{-3}$	$4.6\cdot10^{-3}$	$1.0\cdot10^{-4}$	$1.1\cdot10^{-2}$	$1.1\cdot10^{-4}$	$7.0\cdot10^{-5}$	-0.79	-3.23
BB29-12/2-4	72.5	19.9	25.10	8	$1.8\cdot10^{-3}$	$2.2\cdot10^{-3}$	$7.9\cdot10^{-3}$	$1.4\cdot10^{-4}$	$1.2\cdot10^{-2}$	$1.8\cdot10^{-4}$	$1.5\cdot10^{-4}$	-0.49	-2.97
BB29-11/2-1	66	16.3	29.54	8.1	$2.0\cdot10^{-3}$	$1.4\cdot10^{-3}$	$9.8\cdot10^{-3}$	$1.6\cdot10^{-4}$	$1.3\cdot10^{-2}$	$2.1\cdot10^{-4}$	$2.0\cdot10^{-4}$	-0.25	-3.05
BB29-11/2-2	61	15.2	31.32	7.9	$1.8\cdot10^{-3}$	$1.8\cdot10^{-3}$	1.010^{-2}	$1.8\cdot10^{-4}$	$1.3\cdot10^{-2}$	$2.3\cdot10^{-4}$	$2.3\cdot10^{-4}$	-0.41	-2.89
BB29-11/2-3	56	14.2	33.17	8.1	$2.0\cdot10^{-3}$	$2.0\cdot10^{-3}$	$9.8\cdot10^{-3}$	$1.8\cdot10^{-4}$	$1.3\cdot10^{-2}$	$2.2\cdot10^{-4}$	$2.0\cdot10^{-4}$	-0.22	-2.89
BB29-11/2-4	51	14.2	33.17	8.2	$2.5\cdot10^{-3}$	$2.2\cdot10^{-3}$	$8.9\cdot10^{-3}$	$1.7\cdot10^{-4}$	$1.2\cdot10^{-2}$	$1.4\cdot10^{-4}$	$1.3\cdot10^{-4}$	-0.23	-3.05

Table 4. Chemical composition (in mol/L) of 1:4 aqueous extracts from bentonite samples at different radial distances along section 19. Also listed are dilution factors, *F*, defined in Equation 4 and saturation index with respect to gypsum.

Sample	Radial distance (cm)	w.c. (%)	Dilution factor	pH	HCO_3^-	SO_4^{2-}	Cl^-	K^+	Na^+	Mg^{2+}	Ca^{2+}	SI Gypsum
BB19-14/1	90.67	22.1	23.10	8.13	$1.8\cdot10^{-3}$	$2.2\cdot10^{-3}$	$3.5\cdot10^{-3}$	$1.2\cdot10^{-4}$	$9.9\cdot10^{-3}$	$1.0\cdot10^{-4}$	$7.3\cdot10^{-5}$	-3.29
BB19-14/2	87	21.8	23.35	8.10	$1.9\cdot10^{-3}$	$2.1\cdot10^{-3}$	$3.7\cdot10^{-3}$	$1.2\cdot10^{-4}$	$9.7\cdot10^{-3}$	$1.1\cdot10^{-4}$	$7.0\cdot10^{-5}$	-3.33
BB19-14/3	83.33	22.1	23.10	8.17	$1.8\cdot10^{-3}$	$2.0\cdot10^{-3}$	$4.5\cdot10^{-3}$	$1.5\cdot10^{-4}$	$1.0\cdot10^{-2}$	$1.1\cdot10^{-4}$	$9.0\cdot10^{-5}$	-3.25
BB19-14/4-4	79.67	21.1	23.96	8.03	$1.7\cdot10^{-3}$	$2.1\cdot10^{-3}$	$5.5\cdot10^{-3}$	$1.4\cdot10^{-4}$	$1.1\cdot10^{-2}$	$1.3\cdot10^{-4}$	$1.2\cdot10^{-4}$	-3.12
BB19-14/5	76	21.2	23.87	8.13	$1.7\cdot10^{-3}$	$2.2\cdot10^{-3}$	$5.9\cdot10^{-3}$	$1.5\cdot10^{-4}$	$1.1\cdot10^{-2}$	$1.5\cdot10^{-4}$	$1.4\cdot10^{-4}$	-3.01
BB19-14/6	72.33	20.8	24.23	8	$1.7\cdot10^{-3}$	$2.1\cdot10^{-3}$	$6.4\cdot10^{-3}$	$1.6\cdot10^{-4}$	$1.2\cdot10^{-2}$	$1.6\cdot10^{-4}$	$1.6\cdot10^{-4}$	-2.95
BB19-15/1	68.67	18.6	26.51	8	$1.9\cdot10^{-3}$	$1.8\cdot10^{-3}$	$6.6\cdot10^{-3}$	$1.4\cdot10^{-4}$	$1.2\cdot10^{-2}$	$1.5\cdot10^{-4}$	$1.5\cdot10^{-4}$	-3.07
BB19-15/2	65	18.0	27.22	8.03	$1.9\cdot10^{-3}$	$1.8\cdot10^{-3}$	$7.2\cdot10^{-3}$	$1.6\cdot10^{-4}$	$1.1\cdot10^{-2}$	$1.4\cdot10^{-4}$	$1.5\cdot10^{-4}$	-3.08
BB19-15/3	61.33	17.4	27.99	7.95	$2.0\cdot10^{-3}$	$2.1\cdot10^{-3}$	$6.0\cdot10^{-3}$	$1.6\cdot10^{-4}$	$1.1\cdot10^{-2}$	$1.5\cdot10^{-4}$	$1.7\cdot10^{-4}$	-2.94
BB19-15/4	57.66	17.2	28.26	8	$2.1\cdot10^{-3}$	$1.7\cdot10^{-3}$	$6.4\cdot10^{-3}$	$1.5\cdot10^{-4}$	$1.1\cdot10^{-2}$	$1.3\cdot10^{-4}$	$1.4\cdot10^{-4}$	-3.11
BB19-15/5	53.99	16.4	29.39	8	$2.2\cdot10^{-3}$	$1.6\cdot10^{-3}$	$6.5\cdot10^{-3}$	$1.7\cdot10^{-4}$	$1.1\cdot10^{-2}$	$1.1\cdot10^{-4}$	$1.5\cdot10^{-4}$	-3.12
BB19-15/6	50.32	16.5	29.24	7.97	$2.2\cdot10^{-3}$	$1.8\cdot10^{-3}$	$5.9\cdot10^{-3}$	$1.7\cdot10^{-4}$	$1.1\cdot10^{-2}$	$4.8\cdot10^{-5}$	$1.7\cdot10^{-4}$	-3.01

Table 5. Calculated and measured 1:4 aqueous extract concentrations for bentonite sample BB29-11/2-3 of section 29. Also listed are calculated and inferred concentrations for the original sample at a gravimetric water content of 14.2 % for the base run and sensitivity runs to changes in protolysis constants and types of sorption sites (concentrations in mol/L).

	pH	HCO_3^-	SO_4^{2-}	Cl^-	K^+	Na^+	Mg^{2+}	Ca^{2+}
Measured	8.1	$2.0\cdot10^{-3}$	$2.0\cdot10^{-3}$	$9.8\cdot10^{-3}$	$1.8\cdot10^{-4}$	$1.3\cdot10^{-2}$	$2.2\cdot10^{-4}$	$2.0\cdot10^{-4}$
Base run with 1-type of sorption sites. Protolysis constants: Log K_{int} = -5.8 for XOH_2^+ and Log K_{int} = 11.8 for XO^-								
Inferred	7.85	$3.6\cdot10^{-4}$	$4.2\cdot10^{-2}$	$3.3\cdot10^{-1}$	$1.8\cdot10^{-3}$	$1.3\cdot10^{-1}$	$2.8\cdot10^{-2}$	$2.6\cdot10^{-2}$
Calculated	8.3	$2.1\cdot10^{-3}$	$1.9\cdot10^{-3}$	$9.8\cdot10^{-3}$	$1.7\cdot10^{-4}$	$1.3\cdot10^{-2}$	$2.2\cdot10^{-4}$	$2.0\cdot10^{-4}$
Sensitivity run with 1-type of sorption sites. Protolysis constants: Log K_{int} = -5 for XOH_2^+ and Log K_{int} = 8.7 for XO^-								
Inferred	8.0	$1.14\cdot10^{-4}$	$4.2\cdot10^{-2}$	$3.3\cdot10^{-1}$	$1.6\cdot10^{-3}$	$1.28\cdot10^{-1}$	$2.9\cdot10^{-2}$	$2.8\cdot10^{-2}$
Calculated	8.9	$1.7\cdot10^{-3}$	$1.9\cdot10^{-3}$	$9.8\cdot10^{-3}$	$1.5\cdot10^{-4}$	$1.25\cdot10^{-2}$	$2.4\cdot10^{-4}$	$2.3\cdot10^{-4}$
Sensitivity run with 3-types of sorption sites. Protolysis constants from Bradbury and Baeyens (1997)								
Calculated	9.1	$1.4\cdot10^{-3}$	$1.9\cdot10^{-3}$	$9.8\cdot10^{-3}$	$1.3\cdot10^{-4}$	$1.2\cdot10^{-2}$	$1.9\cdot10^{-4}$	$1.8\cdot10^{-4}$

Table 6. Calculated and measured 1:4 aqueous extract concentrations for bentonite sample BB19-14/5 of section 19. Also listed are concentrations inferred for the original sample at a gravimetric water content of 21.2 % (concentrations in mol/L).

	pH	HCO_3^-	SO_4^{2-}	Cl^-	K^+	Na^+	Mg^{2+}	Ca^{2+}
Measured	8.1	$1.7\cdot10^{-3}$	$2.2\cdot10^{-3}$	$5.9\cdot10^{-3}$	$1.5\cdot10^{-4}$	$1.1\cdot10^{-2}$	$1.5\cdot10^{-4}$	$1.4\cdot10^{-4}$
Inferred	7.88	$6.4\cdot10^{-4}$	$5.2\cdot10^{-2}$	$1.4\cdot10^{-1}$	$1.3\cdot10^{-3}$	$9.1\cdot10^{-2}$	$1.4\cdot10^{-2}$	$1.2\cdot10^{-2}$
Calculated	8.4	$3.2\cdot10^{-3}$	$2.2\cdot10^{-3}$	$5.9\cdot10^{-3}$	$1.5\cdot10^{-4}$	$1.2\cdot10^{-2}$	$1.5\cdot10^{-4}$	$1.4\cdot10^{-4}$

Table 7. Inferred chemical composition (in mol/L) of 1:4 aqueous extracts from bentonite samples at different radial distances along section 29.

Sample	Dist. (cm)	w.c. (%)	pH	HCO_3^-	SO_4^{2-}	Cl^-	K^+	Na^+	Mg^{2+}	Ca^{2+}
BB29-7/1-10	97.5	26.5	8.08	$8.66\cdot10^{-4}$	$3.26\cdot10^{-2}$	$1.64\cdot10^{-2}$	$2.86\cdot10^{-4}$	$3.25\cdot10^{-2}$	$1.38\cdot10^{-3}$	$4.13\cdot10^{-3}$
BB29-12/2-1	87.5	21	8.11	$9.80\cdot10^{-4}$	$6.76\cdot10^{-2}$	$4.00\cdot10^{-2}$	$4.11\cdot10^{-4}$	$4.50\cdot10^{-2}$	$3.07\cdot10^{-3}$	$4.89\cdot10^{-3}$
BB29-12/2-2	82.5	22	8.02	$9.47\cdot10^{-4}$	$7.07\cdot10^{-2}$	$4.97\cdot10^{-2}$	$5.26\cdot10^{-4}$	$4.89\cdot10^{-2}$	$5.11\cdot10^{-3}$	$5.35\cdot10^{-3}$
BB29-12/2-3	77.5	20.3	7.90	$7.54\cdot10^{-4}$	$6.56\cdot10^{-2}$	$1.14\cdot10^{-1}$	$6.59\cdot10^{-4}$	$6.47\cdot10^{-2}$	$6.69\cdot10^{-3}$	$8.69\cdot10^{-3}$
BB29-12/2-4	72.5	19.9	7.88	$4.83\cdot10^{-4}$	$4.83\cdot10^{-2}$	$1.98\cdot10^{-1}$	$8.49\cdot10^{-4}$	$7.59\cdot10^{-2}$	$1.10\cdot10^{-2}$	$1.61\cdot10^{-2}$
BB29-11/2-1	66	16.3	7.81	$3.55\cdot10^{-4}$	$3.84\cdot10^{-2}$	$2.90\cdot10^{-1}$	$1.57\cdot10^{-3}$	$1.27\cdot10^{-1}$	$2.83\cdot10^{-2}$	$2.77\cdot10^{-2}$
BB29-11/2-2	61	15.2	7.81	$3.48\cdot10^{-4}$	$3.82\cdot10^{-2}$	$3.27\cdot10^{-1}$	$1.79\cdot10^{-3}$	$1.25\cdot10^{-1}$	$2.83\cdot10^{-2}$	$2.85\cdot10^{-2}$
BB29-11/2-3	56	14.2	7.85	$3.59\cdot10^{-4}$	$4.22\cdot10^{-2}$	$3.26\cdot10^{-1}$	$1.80\cdot10^{-3}$	$1.30\cdot10^{-1}$	$2.77\cdot10^{-2}$	$2.58\cdot10^{-2}$
BB29-11/2-4	51	14.2	7.93	$5.05\cdot10^{-4}$	$6.54\cdot10^{-2}$	$2.95\cdot10^{-1}$	$1.68\cdot10^{-3}$	$1.15\cdot10^{-1}$	$1.85\cdot10^{-2}$	$1.57\cdot10^{-2}$

Table 8. Inferred chemical composition (in mol/L) of 1:4 aqueous extracts from bentonite samples at different radial distances along section 19.

Sample	Radial distance (cm)	w.c. (%)	pH	HCO_3^-	SO_4^{2-}	Cl^-	K^+	Na^+	Mg^{2+}	Ca^{2+}
BB19-14/1	90.67	22.1	8.12	$9.78\cdot10^{-4}$	$5.05\cdot10^{-2}$	$8.07\cdot10^{-2}$	$6.44\cdot10^{-4}$	$5.23\cdot10^{-2}$	$4.97\cdot10^{-3}$	$4.27\cdot10^{-3}$
BB19-14/2	87	21.8	8.13	$9.95\cdot10^{-4}$	$4.97\cdot10^{-2}$	$8.61\cdot10^{-2}$	$5.94\cdot10^{-4}$	$5.04\cdot10^{-2}$	$4.88\cdot10^{-3}$	$4.07\cdot10^{-3}$
BB19-14/3	83.33	22.1	8.07	$8.78\cdot10^{-4}$	$4.56\cdot10^{-2}$	$1.03\cdot10^{-1}$	$8.87\cdot10^{-4}$	$6.05\cdot10^{-2}$	$5.99\cdot10^{-3}$	$5.09\cdot10^{-3}$
BB19-14/4-4	79.67	21.1	7.98	$7.72\cdot10^{-4}$	$4.94\cdot10^{-2}$	$1.33\cdot10^{-1}$	$9.73\cdot10^{-4}$	$7.52\cdot10^{-2}$	$9.46\cdot10^{-3}$	$7.55\cdot10^{-3}$
BB19-14/5	76	21.2	7.88	$6.36\cdot10^{-4}$	$5.17\cdot10^{-2}$	$1.42\cdot10^{-1}$	$1.25\cdot10^{-3}$	$9.12\cdot10^{-2}$	$1.41\cdot10^{-2}$	$1.21\cdot10^{-2}$
BB19-14/6	72.33	20.8	7.82	$5.50\cdot10^{-4}$	$5.15\cdot10^{-2}$	$1.55\cdot10^{-1}$	$1.34\cdot10^{-3}$	$9.80\cdot10^{-2}$	$1.66\cdot10^{-2}$	$1.55\cdot10^{-2}$
BB19-15/1	68.67	18.6	7.82	$5.77\cdot10^{-4}$	$4.83\cdot10^{-2}$	$1.74\cdot10^{-1}$	$1.30\cdot10^{-3}$	$1.02\cdot10^{-1}$	$1.66\cdot10^{-2}$	$1.56\cdot10^{-2}$
BB19-15/2	65	18.0	7.81	$5.69\cdot10^{-4}$	$4.85\cdot10^{-2}$	$1.96\cdot10^{-1}$	$1.50\cdot10^{-3}$	$1.08\cdot10^{-1}$	$1.76\cdot10^{-2}$	$1.66\cdot10^{-2}$
BB19-15/3	61.33	17.4	7.80	$5.37\cdot10^{-4}$	$4.74\cdot10^{-2}$	$1.69\cdot10^{-1}$	$1.43\cdot10^{-3}$	$1.03\cdot10^{-1}$	$1.70\cdot10^{-2}$	$1.77\cdot10^{-2}$
BB19-15/4	57.66	17.2	7.81	$5.75\cdot10^{-4}$	$4.92\cdot10^{-2}$	$1.82\cdot10^{-1}$	$1.44\cdot10^{-3}$	$1.09\cdot10^{-1}$	$1.65\cdot10^{-2}$	$1.61\cdot10^{-2}$
BB19-15/5	53.99	16.4	7.81	$5.66\cdot10^{-4}$	$4.79\cdot10^{-2}$	$1.90\cdot10^{-1}$	$1.70\cdot10^{-3}$	$1.00\cdot10^{-1}$	$1.36\cdot10^{-2}$	$1.62\cdot10^{-2}$
BB19-15/6	50.32	16.5	7.81	$5.41\cdot10^{-4}$	$4.43\cdot10^{-2}$	$1.74\cdot10^{-1}$	$1.60\cdot10^{-3}$	$9.70\cdot10^{-2}$	$5.49\cdot10^{-3}$	$1.66\cdot10^{-2}$

Table 9. Calculated and measured 1:4 aqueous extract concentrations for bentonite sample BB29-11/2-3 of section 29 for base run and a sensitivity run with an initial amount of gypsum (concentrations in mol/L).

	pH	HCO_3^-	SO_4^{2-}	Cl^-	K^+	Na^+	Mg^{2+}	Ca^{2+}
Measured	8.1	$2.0\cdot10^{-3}$	$2.0\cdot10^{-3}$	$9.8\cdot10^{-3}$	$1.8\cdot10^{-4}$	$1.3\cdot10^{-2}$	$2.2\cdot10^{-4}$	$2.0\cdot10^{-4}$
Base run: no gypsum initially								
Inferred	7.85	$3.6\cdot10^{-4}$	$4.2\cdot10^{-2}$	$3.3\cdot10^{-1}$	$1.8\cdot10^{-3}$	$1.3\cdot10^{-1}$	$2.8\cdot10^{-2}$	$2.6\cdot10^{-2}$
Calculated	8.3	$2.1\cdot10^{-3}$	$1.9\cdot10^{-3}$	$9.8\cdot10^{-3}$	$1.7\cdot10^{-4}$	$1.3\cdot10^{-2}$	$2.2\cdot10^{-4}$	$2.0\cdot10^{-4}$
Sensitivity run: 0.08 % initial volume fraction of gypsum								
Inferred	7.85	$3.6\cdot10^{-4}$	$6.6\cdot10^{-5}$	$3.3\cdot10^{-1}$	$2.3\cdot10^{-5}$	$5.1\cdot10^{-1}$	$1.1\cdot10^{-3}$	$1.7\cdot10^{-1}$
Calculated	8.3	$5.6\cdot10^{-4}$	$5.7\cdot10^{-2}$	$9.8\cdot10^{-3}$	$5.3\cdot10^{-6}$	$1.2\cdot10^{-2}$	$1.2\cdot10^{-4}$	$1.2\cdot10^{-2}$

Table 10. Sensitivity analysis of model results of BB29-11/2-3 to surface complexation and calcite dissolution.

	pH	HCO_3^-	SO_4^{2-}	Cl^-	K^+	Na^+	Mg^{2+}	Ca^{2+}
Initial concentrations	7.85	$3.6\cdot10^{-4}$	$4.2\cdot10^{-2}$	$3.3\cdot10^{-1}$	$1.8\cdot10^{-3}$	$1.3\cdot10^{-1}$	$2.8\cdot10^{-2}$	$2.6\cdot10^{-2}$
Measured	8.1	$2.0\cdot10^{-3}$	$2.0\cdot10^{-3}$	$9.8\cdot10^{-3}$	$1.8\cdot10^{-4}$	$1.3\cdot10^{-2}$	$2.2\cdot10^{-4}$	$2.0\cdot10^{-4}$
Calculated with base run	8.3	$2.1\cdot10^{-3}$	$1.9\cdot10^{-3}$	$9.8\cdot10^{-3}$	$1.7\cdot10^{-4}$	$1.3\cdot10^{-2}$	$2.2\cdot10^{-4}$	$2.0\cdot10^{-4}$
Calculated by dropping surface complexation	9.3	$1.2\cdot10^{-3}$	$2.0\cdot10^{-3}$	$9.8\cdot10^{-3}$	$1.4\cdot10^{-4}$	$1.0\cdot10^{-2}$	$1.4\cdot10^{-4}$	$1.4\cdot10^{-4}$
Calculated by dropping both surface complexation and calcite	5.9	$5.8\cdot10^{-5}$	$2.0\cdot10^{-3}$	$9.8\cdot10^{-3}$	$1.0\cdot10^{-4}$	$8.0\cdot10^{-3}$	$7.9\cdot10^{-4}$	$6.9\cdot10^{-5}$